



RESEARCH ARTICLE

Path planning method for unmanned underwater vehicles eliminating effect of currents based on artificial potential field

Danjie Zhu,* and Simon X. Yang

Laboratory of Advanced Robotics and Intelligent System (ARIS), School of Engineering, University of Guelph, Guelph, ON, Canada N1G2W1.

*Corresponding author. E-mail: danjie@uoguelph.ca

Received: 1 January 2021; **Accepted:** 15 March 2021; **First published online:** 14 April 2021

Keywords: artificial potential field, currents effect, optimal path planning, unmanned underwater vehicles

Abstract

To eliminate the effect of ocean currents for optimal path planning for unmanned underwater vehicles (UUVs) in the underwater environment, an intelligent algorithm is designed and proposed in this paper. The algorithm consists of two parts: an artificial potential field-based algorithm that derives the shortest path and avoids collision accidents; and an adjusting function that eliminates the effect of ocean currents. The planning results of the intelligent algorithm are presented in detail, and compared with the conventional algorithm that does not consider the effect of currents. The effectiveness of the optimised path planning method given in this paper is proved.

1. Introduction

Abundant resources embedded in the ocean area, such as biological resources, mineral resources and space resources, are still waiting to be explored (Hovem et al., 2014; Hu et al., 2015). Therefore, attention has been attracted to the field of undersea exploration for decades (Gafurov and Klochkov, 2015; Emami and Taban, 2018). Among the technologies that are beneficial for marine exploration, detection by unmanned underwater vehicle (UUV) is one of the most significant and applicable technologies. For effective underwater operation of UUVs, the path planning problem is worthy of thorough study (Zhu et al., 2018; Hu et al., 2019). Considering the complex condition of deep-water areas, such as the invisibility and irregularity of obstacles, the ability of UUVs to navigate with an in-time reaction to avoid collisions and to address the optimal path between the starting and ending point is very important (Singh et al., 2018; Yu and Su, 2001). Generally, the path planning process of the UUV is to start from an initial position, then search along the shortest path or in the shortest time to reach the destination (Panda et al., 2019). During the searching process all the possible obstacles should be avoided. In the underwater environment, where ocean currents commonly exist, the UUV usually deviates from the optimal path due to the effect of the currents, thus leading to waste of time and energy (Aghababa, 2012; Cao et al., 2019). For instance, without considering the ocean currents from a direction that drags the UUV away from its destination, the vehicle may travel along a longer path or take a longer time.

Researchers have devoted efforts to the study of finding the optimal path for unmanned vehicles since the mid twentieth century (Cao et al., 2019; Li et al., 2019a, 2019b; Wang et al., 2020). Various intelligent methods have been raised, but most of them are based on the grid modelling of the environment, where the environmental factors are formalised into smallest cells to establish the complete model. For example, the Dijkstra algorithm was applied to the path planning problem at the earliest stage, but it

needs to search through all the possible paths that are connected by the grid-based nodes to address the optimal solution with the shortest distance (Dijkstra, 1959). The A* method was introduced later to improve the efficiency of the path finding process by adding the heuristic cost to the nodes, thus largely reducing the searching space (Hart et al., 1968). Refined A* method has also been applied in the marine system with the effect of currents and moving obstacles involved in the experiment (Singh et al., 2018).

However, the underwater environment produces higher complexity for these grid-based methods, as the randomly distributed and irregular-shaped obstacles, as well as the dynamics of fluids, require more time and energy to form a model with acceptable accuracy (Yu et al., 2020). The artificial potential field (APF) alleviates the problem without the requirement of grid-based modelling (Khatib, 1986). APF reduces the calculation complexity as well as performing outstanding real-time reactions, making it widely applied in the area of vehicle path planning. The virtual gravitational potential field realises the rapid address of the optimal path without collisions for robot manipulators, following the guidance of resultant forces given by the pre-designed attraction and repulsion (Ralli and Hirzinger, 1994). Zhou and colleagues improved the APF method with particle swarm algorithm to increase the path finding efficiency for tangent navigating robots (Zhou et al., 2018). The path planning problem of multi-rotor unmanned vehicles has been resolved through the combination of the APF and biogeography based method (Song et al., 2019). Lin and colleagues designed a subgoal algorithm to the APF such that the path planning of the unmanned vehicle can overcome the local minimum and track the optimal path (Lin et al., 2019). Decision tree has been added to the APF to form an efficient path planning algorithm without local minimum and avoiding collisions for the vehicles (Lin et al., 2020). Most of the APF research, however, does not involve the environmental disturbance in the design, thus affecting the practical application of APF. Especially for the UUV path planning, inevitable deviation brought by the effect of ocean currents cannot be neglected, which is the motivation of the improved APF method proposed in this paper.

In this paper, an intelligent path planning algorithm based on the theory of APF that eliminates the effect of ocean currents on UUV is proposed. Obstacles are supposed to create repulsion from the vehicle while the destination attracts the vehicle. Therefore a virtual potential field is established, according to the decrease of the gravitational field; the optimal path can be addressed and meanwhile the avoidance of obstacles realised throughout the whole process. Most importantly, the deviation brought by the effect of ocean currents is eliminated by adjusting the heading direction and velocity produced by the UUV at each step, thus sustaining the vehicle to track the optimal path consistently. In the second section of the paper, the underwater path planning problem for the UUV is described, the corresponding model is established, and the proposed APF-based path planning method is explained in detail. In the third section, simulation results of the proposed path planning algorithm and the conventional method that does not eliminate the effect of currents are demonstrated and compared in detail, where the effectiveness of the proposed approach with current effects eliminated is proved.

2. Problem statement and the proposed path planning algorithm design

In this section, the proposed method that deduces the optimal path for the UUV in two-dimensional (2D) and three-dimensional (3D) underwater environments based on the theory of APF is explained in detail.

2.1. Modelling of the underwater path planning problem

In this study, the underwater environment of the UUV is considered as a 2D or 3D workspace, whose dimensions vary according to the requirements of the simulation. The obstacles in the environment are represented by black circles (black spheres for 3D space) randomly distributed in the space, where the radii of all the circles are set at one for computational convenience (see Figure 1). For the path planning problem in the underwater environment, the positions of the vehicle origin and its supposed destination are known at the beginning. The task of the path planning algorithm is to find the optimal path between

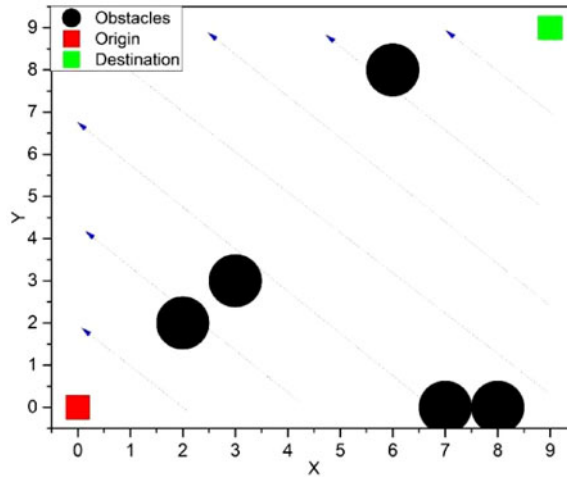


Figure 1. Modelling of the 2D underwater environment for UUV path planning.

the origin and the destination, by avoiding all the obstacle circles and travelling as short a distance as possible.

In the practical case of UUV navigation, the effects of ocean currents of complex fluid status cannot be neglected. Flow from various directions and of different rates brings uncontrollable deviation to the vehicle navigation, thus resulting in the failure of the navigation. Therefore, changing directions and velocities are extracted as the two main characteristics of the ocean currents, and tuned in the simulation to evaluate the effectiveness of the proposed method when applied in the corresponding underwater environment. The direction of the current in the 2D model is represented by blue arrows marked on the map (Figure 1).

2.2. Path planning algorithm design

In response to the requirement of eliminating the effect of ocean currents for the UUV path planning, the current effect-eliminated APF (CAPF) path planning algorithm is designed. The CAPF algorithm consists of two parts: (1) an APF algorithm component that gives the shortest path between the origin and the destination meanwhile avoiding all the obstacles; (2) an adjusting algorithm component that eliminates the deviation created by the effect of the ocean currents.

2.2.1. APF path planning algorithm

Based on the model defined in the previous section, a virtual APF can be established correspondingly. The proposed destination is determined as the object that has attraction to the vehicle, while the obstacles are regarded as objects that generate repulsive force to the vehicle. All the attractive and repulsive forces are quantified and presented in the form of gravity, where positive gravity is correlated with the distance between the vehicle’s position and the destination and negative gravity occurs within the covering range of the obstacles.

The attractive field is defined as,

$$U_{att}(x) = \frac{1}{2}k_{att} \rho^2(x, x_d). \tag{1}$$

where k_{att} is a constant coefficient used to adjust the accuracy of the target attraction on the vehicle; $\rho(x, x_d)$ represents the distance between the current position x and the destination position x_d .

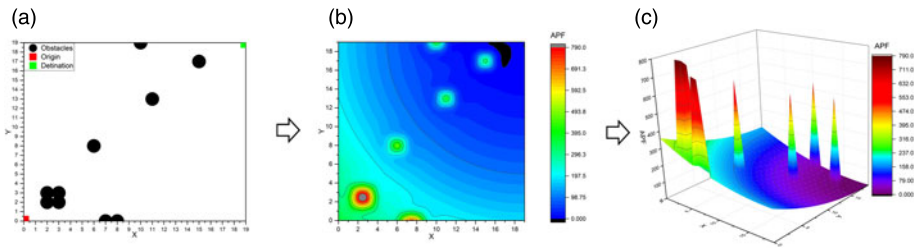


Figure 2. 2D modelling of APF. (a) 2D map of a predefined underwater environment, (b) contour of the map after APF applied, (c) distribution of the APF on the map.

The repulsive field is,

$$U_{att}(x) = \begin{cases} \frac{1}{2} k_{rep} \left(\frac{1}{\rho(x, x_o)} - \frac{1}{\rho_o} \right)^2, & \rho(x, x_d) < \rho_o \\ 0, & \rho(x, x_d) \geq \rho_o \end{cases} \tag{2}$$

where the k_{rep} is the constant coefficient for tuning the repulsive effect to the vehicle; $\rho(x, x_o)$ represents the distance between the current position x and the obstacle position x_o ; ρ_o is the radius of the obstacle, all of which are set at one in this study.

Once the attractive and repulsive field are defined, the virtual potential field of the whole map can be addressed (see Figure 2). As the vehicle moves closer to the destination, the gravity decreases until it reaches the destination. Therefore the destination has the lowest gravity field but the highest gravity force for attraction (Figure 2(b) and (c)). The gravity field for the obstacles is higher such that they repulse the vehicle from approaching (Figure 2(b) and (c)).

Planning a path between the vehicle’s origin and its destination is based on the established virtual field, whose heading direction and step magnitude are addressed through attractive and repulsive forces. These forces are achieved by taking derivatives of the predefined fields (Equations (1) and (2)),

$$\begin{aligned} F_{att}(x) &= -\nabla U_{att}(x) = k_{att} \rho(x, x_d) \\ F_{rep}(x) &= -\nabla U_{rep}(x) \\ &= \begin{cases} k_{rep} \left(\frac{1}{\rho(x, x_o)} - \frac{1}{\rho_o} \right) \frac{1}{\rho^2(x, x_o)} \nabla \rho(x, x_o), & \rho(x, x_d) < \rho_o \\ 0, & \rho(x, x_d) \geq \rho_o \end{cases} \end{aligned} \tag{3}$$

Therefore the summation of the force can be obtained to give instructions on finding the optimal path without collisions,

$$F(x) = F_{att}(x) + F_{rep}(x) = -\nabla U(x) \tag{4}$$

Step positions for the path planning are addressed and are correlated after reaching the destination to form the final optimal path solution (see Figure 3).

2.2.2. Elimination of the effects of currents

The choice of the next position along the ideal path is based on the current position of the vehicle. In other words, the optimal path can be formed periodically and correlated afterwards, which is the same for the effect of currents, as given in Figure 4. It is clearly shown that the difference between the direction of the ocean currents velocity v_{cur} and the direction of the vehicle’s desired velocity v_d obviously affects the navigational trajectory of the vehicle at each position, thus resulting in the large deviation from the optimal path v_{act} after accumulation.

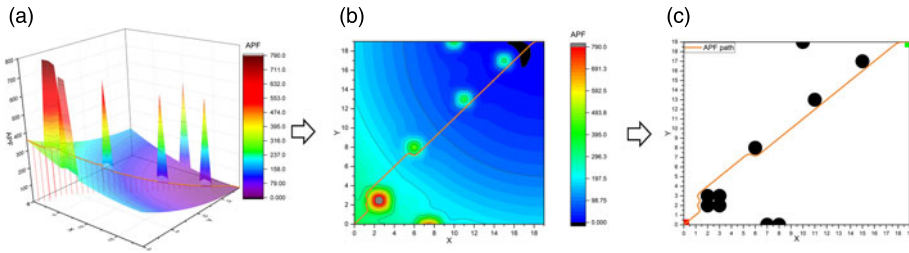


Figure 3. Path derived by the APF method on the 2D modelling map. (a) path planning based on the distribution of the APF on the map, (b) APF path on the contour map, (c) final APF path presented on the 2D modelling map.

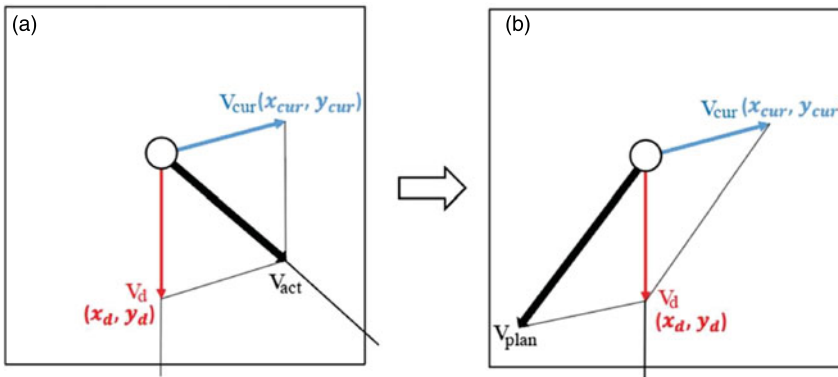


Figure 4. Elimination of the effect of ocean currents by introducing a third party velocity vector.

To eliminate the deviation, a third party velocity vector given by the vehicle, the planned velocity vector v_{plan} , is derived based on the parallelogram law (see Figure 4(b)). In Figure 4(b), summation of v_{cur} and v_{plan} results in v_d , which allows the vehicle to travel in the desired direction with the desired velocity. The current velocity vector v_{cur} is obtained from the environment. The specific direction of the desired velocity vector v_d is derived by the optimal path, based on the intelligent path planning algorithm proposed in this paper. Additionally, the size of v_d is set at the beginning.

As the sizes of v_d and v_{cur} are known, suppose the position of v_d is (x_d, y_d) , and v_{cur} is (x_{cur}, y_{cur}) ; then the position of the planned velocity vector v_{plan} can be attained based on the parallelogram law (see Figure 4(b)),

$$v_{plan} : (x_d - x_{cur}, y_d - y_{cur}) \tag{5}$$

When extended to the 3D model, a similar mechanism is applied where the third party velocity vector v_{plan} is introduced with an extra dimension added. According to the parallelogram law, v_{plan} balances the effect brought by the ocean currents vector v_{cur} and finally gives the result corresponding to the desired velocity vector v_d to follow the optimal planning path. The precise direction and size of v_{plan} are deducted by the positions of the separate vectors in 3D space. As the direction and speed of v_d and v_{cur} are given, suppose the position of v_d : (x_d, y_d, z_d) , and v_{cur} : $(x_{cur}, y_{cur}, z_{cur})$. The position of v_{plan} can then be obtained similarly on the basis of the parallelogram relationship illustrated in Figure 4(b),

$$v_{plan} : (x_d - x_{cur}, y_d - y_{cur}, z_d - z_{cur}) \tag{6}$$

Therefore v_{plan} is derived to complete the elimination of the effect of ocean currents in the 3D environment.

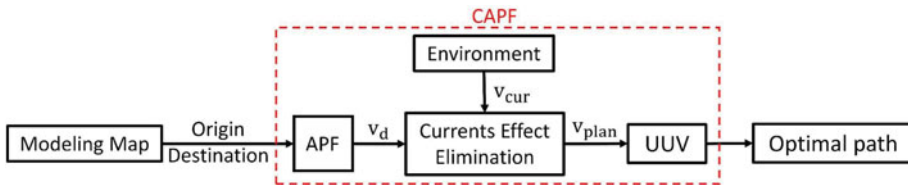


Figure 5. Schematic of the proposed optimal path planning method designed for UUV in the underwater environment.

2.2.3. CAPF path planning algorithm

The two separately designed components are combined to obtain a final path planning algorithm that eliminates the effect of currents and sustains the optimal path solution (see Figure 5). The desired velocity and direction computed by the APF algorithm at each position is passed to the elimination component to plan the velocity and direction the UUV should produce. The planned velocity and direction guarantee that the vehicle will travel along the optimal path by eliminating the effect of currents neuron by neuron, thus providing a robust and efficient path planning result for the UUV. The schematic for realising the algorithm is given in Figure 5.

3. Simulation results and analysis

In this section, the path planning results given by the CAPF method and the APF method which does not eliminate the effect of ocean currents are illustrated and analysed. The simulations are tested in conditions of different obstacle-occupied ratios, and currents of different directions and velocities. Additionally, the distances of the planned paths are compared to evaluate the effectiveness of the proposed CAPF algorithm.

3.1. 2D results under currents of different directions

The path planning results in the 2D workspace deduced by the CAPF and the APF algorithm are demonstrated in this section. Input parameters are set at: $v_d = 1$ m/s, $v_{cur} = 0.02$ m/s, $k_{att} = 1$ and $k_{rep} = 50$, which are obtained by trial and error. For the 2D space of size 10×10 , the initial position of the vehicle is set as the origin, whose coordinates are (0, 0). The supposed destination is at (9, 9).

The results of the planned paths under currents of different direction given by the CAPF (in black line) and the conventional APF (in blue dot) algorithm are shown in Figure 6. The velocity of the current is set at 0.02 m/s for all cases, which is to address the greater distance of the APF path to reach the destination. Current directions of 0, 45, 90 and 135 degrees counterclockwise are applied to assess the effect of the fluid flow on the 2D map when tracking the path from the left bottom to the right bottom. The existence of the current, even with a very low flow rate, created inevitable deviation for the paths of the conventional APF algorithm in some of the cases, where in Figure 6(a) and (c) the vehicle fails to reach the destination. The deviation of the paths deduced by the conventional algorithm follows the direction of the current, thus sending the vehicle off-track from the ideal heading direction, and leads to accidental collisions with obstacles (see Figure 6(a) and (c)).

Moreover, compared with the CAPF algorithm, the data from the APF-derived paths show that larger distances were travelled in the navigation between the origin and the destination (see Table 1). This demonstrates that the conventional algorithm does not provide the optimal planning path, which in turn causes the vehicle to consume more energy.

3.2. 2D results under currents of different velocities

To test the effect of the current flow rate on the results, simulations of the CAPF and the conventional APF algorithm under currents of different velocities are presented in Figure 7, with the same parameters

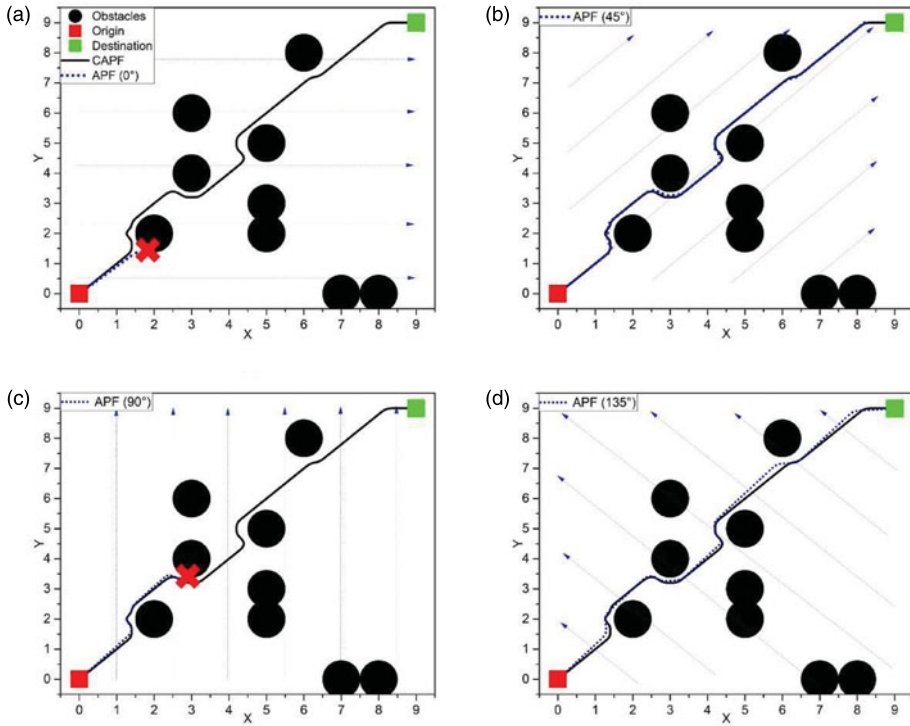


Figure 6. 2D comparison results of the paths given by CAPF algorithm and APF algorithm under currents of different directions. Directions of currents (all counterclockwise): (a) 0 degree, (b) 45 degrees, (c) 90 degrees, (d) 135 degrees.

Table 1. 2D moving results of the two path planning algorithms under currents of different directions.

| Algorithm | Direction of currents (degrees) | | | | |
|-----------|---------------------------------|---------|---------|---------|---------|
| | 0 | 45 | 90 | 135 | 180 |
| CAPF | 14.5137 | 14.5137 | 14.5137 | 14.5137 | 14.5137 |
| APF | C & F | 14.8364 | F | 14.5607 | 14.7025 |

Unit: m, C: Collision, F: Fail to reach the destination.

applied as in the previous section but the current direction is set at 135 degrees counterclockwise for all cases to make a more direct comparison. As the velocity of the current increases, the paths of the APF algorithm (blue dots) deviate accordingly, while the CAPF algorithm (black line) keeps the vehicle navigating along the optimal path without any deviations. For example, when the current velocity is as low as 0.02 m/s, the APF path almost overlaps the optimal path with very small deviation (Figure 7(a)). When the currents velocity increases, for the path of APF algorithm, increasing deviation is produced, which leads to uncontrollable accidents such as collision (Figure 7(b)), failure to reach the destination (Figure 7(c)) and even going off the map at the early stage (Figure 7(d)). At the same time, with the CAPF algorithm, the vehicle always follows the trajectory of the optimal path regardless of the change of the current velocity. This conclusion is also supported by the results listed in Table 2, where the distances of the paths given by the two algorithms are compared. It is clearly shown that the CAPF algorithm always sustains the shortest length path distance of 14.5137 m, while the UUV with APF algorithm has to travel longer distances to reach the destination, and even cannot accomplish the proposed journey due

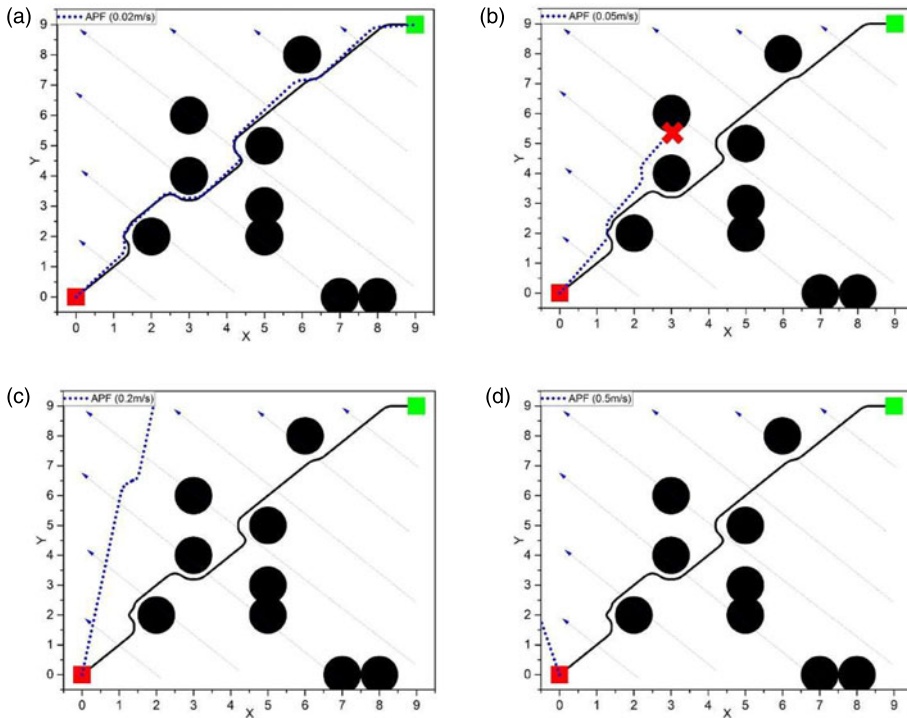


Figure 7. 2D comparison results of the paths given by CAPF algorithm and APF algorithm under currents of different velocities. Velocities of currents: (a) 0.02 m/s, (b) 0.05 m/s, (c) 0.2 m/s, (d) 0.5 m/s.

to the increasing deviation brought by the change of the current velocity. Therefore the CAPF method saves more energy by guaranteeing the optimal navigation for the vehicle when operating in currents of different directions or velocities.

The path planning results under dynamic ocean currents with continuously changing velocities and directions are presented in Figure 8. The path of the APF algorithm (blue dots) vibrates fiercely with the currents' flowing tendency, and finally goes out of control before reaching the destination (see the top-right part in Figure 8). The CAPF algorithm retains the optimal path (black line) throughout the whole process, unaffected by the dynamically changing currents, and exactly overlaps the path derived under the condition without currents (orange stars). This proves the effectiveness of the CAPF algorithm for eliminating the influence of the velocity of currents and shows that it successfully drives and tracks the optimal path between the supposed origin and the destination.

3.3. 2D results under different obstacle-occupied ratios

As the underwater obstacles are distributed randomly in both size and position, the path planning results of different obstacle-occupied ratios are simulated in Figure 9 to evaluate the effectiveness of the CAPF algorithm. The obstacle-occupied ratio means the approximate ratio between the size of all obstacles and the size of the map. The same parameters are applied as in the previous simulation, and the direction of the currents is set as 135 degrees counterclockwise while the obstacle-occupied ratio varies.

With the increment of the obstacles, the conventional APF algorithm (blue dots) tends to introduce more unpredictability during the navigating process. For instance, the APF path successfully reaches the destination with moderate deviation from the optimal path (Figure 9(a)); when the obstacle-occupied ratio rises to 20% in Figure 9(b), the vehicle controlled by the APF algorithm unexpectedly bumps into an obstacle after completing over half of the journey. The effect of the ocean currents weakens the

Table 2. 2D moving results of the two path planning algorithms under currents of different velocities.

| Algorithm | Velocity of currents (m/s) | | | | | | | | | | |
|-----------|----------------------------|---------|---------|---------|---------|---------|---------|---------|---------|---------|---------|
| | 0.02 | 0.05 | 0.1 | 0.2 | 0.3 | 0.4 | 0.5 | 0.6 | 0.7 | 0.8 | 0.9 |
| CAPF | 14.5137 | 14.5137 | 14.5137 | 14.5137 | 14.5137 | 14.5137 | 14.5137 | 14.5137 | 14.5137 | 14.5137 | 14.5137 |
| APF | 14.5607 | C&F | C&F | F | F | F | F | F | F | F | F |

Unit: m, C: Collision, F: Fail to reach the destination.

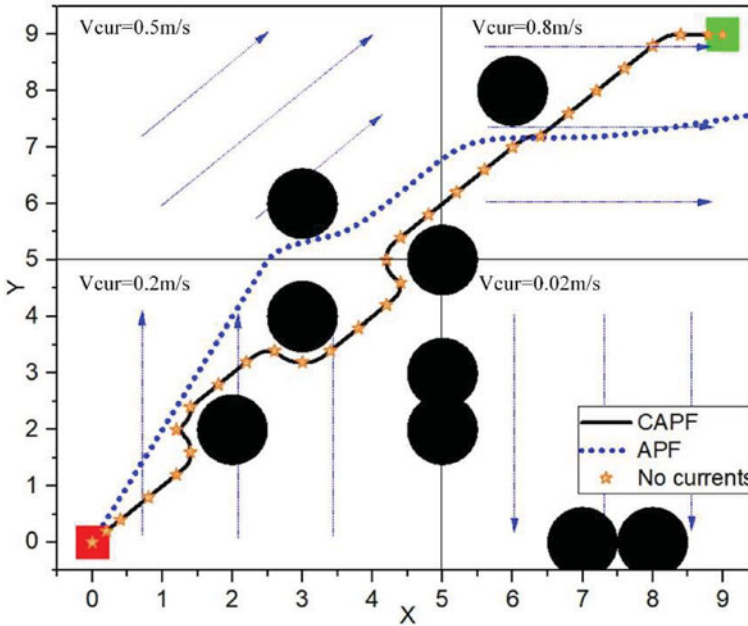


Figure 8. 2D comparison results of the paths given by CAPF algorithm and APF algorithm under dynamic currents. v_{cur} : velocity of currents.

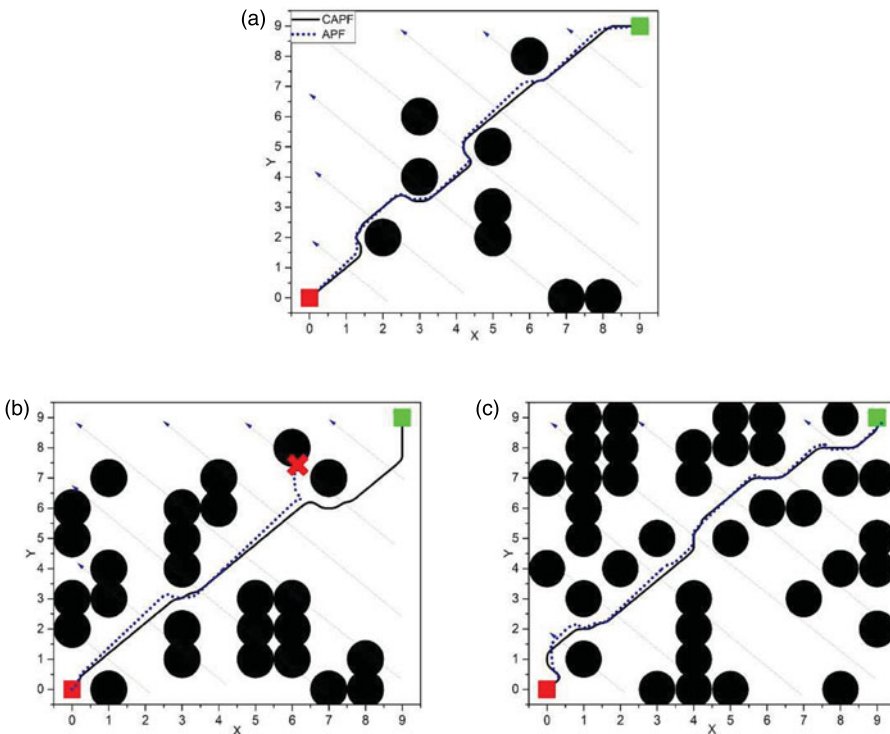


Figure 9. 2D comparison results of the paths given by CAPF algorithm and APF algorithm with different obstacle-occupied ratios: (a) 10% obstacles, (b) 20% obstacles, (c) 40% obstacles.

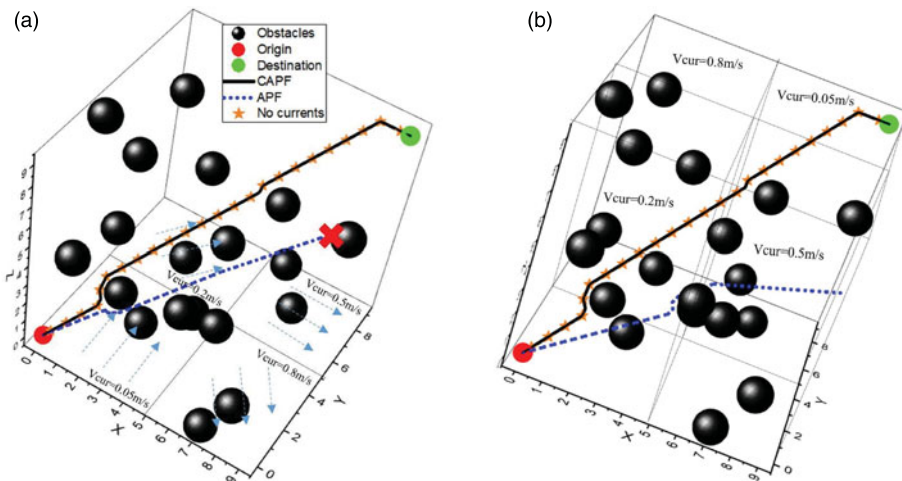


Figure 10. 3D comparison results of the paths given by CAPF algorithm and APF algorithm under dynamic currents. (a) currents in horizontal direction (angle to the X-Y plane: 0 degree, angle to the X-Z plane: see the blue arrow); (b) currents in vertical direction (angle to X-Y plane: 135 degree counterclockwise, angle to the X-Z plane: 0 degree).

supposed obstacle avoidance ability of the vehicle, where the deviated position information accumulates until inevitable accidents such as bumps happen. However, the CAPF algorithm eliminates the effect of the ocean currents and provides correct position information along the whole path. Increasing obstacles do not affect the CAPF algorithm's deduction of the optimal path between the origin and the destination with avoidance of all the possible obstacles (black line). This supports the effectiveness of the proposed algorithm when applied in an underwater environment of randomly distributed obstacles.

3.4. 3D simulation results

Considering that the underwater environment is of three dimensions, the 3D simulation results of the CAPF and the conventional methods are demonstrated. Specific values listed in the previous simulation sections are applied, but the origin is set at (0, 0, 0) and the destination is (9, 9, 9) for 3D modelling. The direction of the ocean currents is determined by two degrees, one is the degree to the X-Y plane, and the other is the degree to the X-Z plane. The size of the 3D workspace is $10 \times 10 \times 10$.

The path planning results of the CAPF (black line) and the conventional APF (blue dots) algorithms under the effect of dynamic currents are given in Figure 10. In Figure 10(a), projections of the partial currents direction are presented on the figure, where all the degrees to the X-Y plane are set to be 0, and the degrees to the X-Z plane are marked by the heading direction of the blue arrows. It is clearly shown that the path of the APF algorithm produces deviation following both the direction and velocity of the partial currents. For example, when the difference between the partial current direction and the supposed heading direction of the vehicle increases, the APF path is dragged farther away from the optimal path and finally cannot reach the destination; the very low flow rate of 0.05 m/s limits the deviation of the APF path at the beginning but inevitable divergence occurs as the partial current velocity grows, which results in collision (red cross) at the end. For Figure 10(b) where vertical currents are applied, the APF path deviates at the very beginning and never reaches the area of the destination. Meanwhile, the changing fluid status of the currents does not affect the optimal path planning of the CAPF algorithm whether the currents come in horizontal or vertical directions, where it exactly corresponds to the optimal path under the non-current condition (orange stars) and avoids all possible collisions throughout the whole process. This proves the effectiveness of the CAPF algorithm at eliminating effect of currents in a 3D environment filled with dynamic fluids, which is applicable for the practical UUV navigation.

4. Conclusion

In this paper, the optimal path planning problem for UUVs under the effect of ocean currents in the underwater environment is discussed. An APF-based algorithm is proposed to eliminate the effect of currents and meanwhile to address the optimal path. A virtual gravitational field is established by supposing the destination as the attraction and the obstacles as the repulsion, thus the optimal path between the origin and the destination can be deduced accordingly. The directions and velocities of ocean currents are characterised as the two major factors that affect the accuracy and safety of UUV navigation along the optimal path. Therefore, based on the parallelogram law, the CAPF algorithm adds an adjusting component for balancing off the deviation brought by the effect of the ocean currents. The simulation results prove that the CAPF algorithm realises the complete elimination of effects of current and the accomplishment of the optimal path with the shortest distance, thus saving more energy for the UUV. The effectiveness of the proposed algorithm is guaranteed in both 2D and 3D conditions under status of changing directions and velocities of currents. In future study, the manoeuvrability problem will be considered when the CAPF algorithm is applied to a vehicle of a specific type and with kinematic/dynamic parameters to improve the adaptiveness of the algorithm in practical applications.

References

- Aghababa, M. (2012). 3D path planning for underwater vehicles using five evolutionary optimization algorithms avoiding static and energetic obstacles. *Application of Ocean Resources*, **38**, 48–62.
- Cao, X., Sun, C.-Y. and Chen, M.-Z. (2019). Path planning for autonomous underwater vehicle in time-varying current. *IEEE Transactions on Intelligent Transportation and System*, **13**(8), 1265–1271.
- Dijkstra, E. (1959). Communication with an automatic computer. Ph.D. thesis, University of Amsterdam, The Netherlands.
- Emami, M. and Taban, M. R. (2018). A low complexity integrated navigation system for underwater vehicles. *Journal of Navigation*, **71**(5), 1161–1177.
- Gafurov, S. and Klochkov, E. (2015). Autonomous unmanned underwater vehicles development tendencies. *Procedia Engineering*, **106**, 141–148.
- Hart, P. E., Nilsson, N. J. and Raphael, B. (1968). A formal basis for the heuristic determination of minimum cost paths. *IEEE Transactions on System, Science and Cybernetics*, **SSC-4**(2), 100–107.
- Hovem, L. A., Torstad, E., Bjerager, P., Bjornsen, T. and Danielsen, H. K. (2014). *Managing Risk in Deepwater Frontiers - Key Learnings from Five Continents*. Moscow, Russia: World Petroleum Congress.
- Hu, C., Wang, R., Yan, F. and Chen, N. (2015). Should the desired heading in path following of autonomous vehicles be the tangent direction of the desired path? *IEEE Transactions on Intelligent Transportation and System*, **16**(6), 3084–3094.
- Hu, Z., Zhu, D., Cui, C. and Sun, B. (2019). Trajectory tracking and re-planning with model predictive control of autonomous underwater vehicles. *Journal of Navigation*, **72**, 321–341.
- Khatib, O. (1986). Real-time obstacle avoidance for manipulators and mobile robots. *International Journal of Robotics Research*, **5**(1), 90–98.
- Li, D., Wang, P. and Du, L. (2019a). Path planning technologies for autonomous underwater vehicles - a review. *IEEE Access*, **7**, 9745–9768.
- Li, B., Zhao, R., Xu, G., Wang, G., Su, Z., and Chen, Z. (2019b) Three-Dimensional Path Planning for an Under-Actuated Autonomous Underwater Vehicle. *Proceedings of the 29th International Ocean and Polar Engineering Conference, Honolulu, Hawaii, USA, June 2019*, 1, 1518–1524.
- Lin, Z., Yue, M., Wu, X. and Tian, H. (2019). An improved artificial potential field method for path planning of mobile robot with subgoal adaptive selection. In Yu, H., Liu, J., Liu, L., Ju, Z., Liu, Y., and Zhou D. (eds), *Intelligent Robotics and Applications. ICIRA 2019*. Lecture Notes in Computer Science, vol 11740. Cham, Switzerland: Springer, pp. 211–220.
- Lin, X., Wang Z.-Q. and Chen X.-Y. (2020). Path Planning with Improved Artificial Potential Field Method Based on Decision Tree. *International Conference on Integrated Navigation Systems (ICINS)*.
- Panda, M., Das, B., Subudhi, B. and Pati, B. (2020). A comprehensive review of path planning algorithms for autonomous underwater vehicles. *International Journal of Autonomous Computation*, **17**(3), 321–352.
- Ralli, E. and Hirzinger, G. (1994). Fast path planning for robot manipulators using numerical potential fields in the configuration space. *IEEE/RSJ/GI International Conference on Intelligent Robots and Systems*, **3**, 1922–1929.
- Singh, Y., Sharma, S., Sutton, R., Hatton, D. and Khan, A. (2018). A constrained a* approach towards optimal path planning for an unmanned surface vehicle in a maritime environment containing dynamic obstacles and ocean currents. *Ocean Engineering*, **169**, 187–201.
- Song, J., Zhao, M., Liu, Y., Liu, H. and Guo, X. (2019). Multi-Rotor UAVs Path Planning Method Based on Improved Artificial Potential Field Method. *Chinese Control Conference (CCC)*, 8242–8247.

- Wang, X., Yao, X. and Zhang, L.** (2020). Path planning under constraints and path following control of autonomous underwater vehicle with dynamical uncertainties and wave disturbances. *Journal of Intelligent and Robotic Systems: Theory and Applications*, **99**(3–4), 891–908.
- Yu, H. and Su, T.** (2001). A destination driven navigator with dynamic obstacle motion prediction. *IEEE International Conference on Robotics and Automation (ICRA)*, **3**, 2692–2697.
- Yu, W., Kin Huat, L. and Chen, L.** (2020). Cooperative path planning for heterogeneous unmanned vehicles in a search-and-track mission aiming at an underwater target. *IEEE Transactions on Vehicular Technology*, **69**(6), 6782–6787.
- Zhou, Z., Wang, J., Zhu, Z., Yang, D. and Wu, J.** (2018). Tangent navigated robot path planning strategy using particle swarm optimized artificial potential field. *Optik*, **158**, 639–651.
- Zhu, D., Liu, Y. and Sun, B.** (2018). Task assignment and path planning of a multi-AUV system based on a Glasius bio-inspired self-organizing map algorithm. *Journal of Navigation*, **71**, 482–496.